Ultrasonics Sonochemistry 30 (2016) 1–8

Contents lists available at ScienceDirect

Ultrasonics Sonochemistry

journal homepage: www.elsevier.com/locate/ultson

Ultrasonic compatibilization of polyelectrolyte complex based on polysaccharides for biomedical applications

M. Soledad Belluzo [a], Lara F. Medina [a,b], Ana M. Cortizo [b], M. Susana Cortizo [a,*]

[a] Instituto de Investigaciones Fisicoquímicas Teóricas y Aplicadas (INIFTA), Universidad Nacional de La Plata, CC 16 Suc. 4, CONICET, CCT-La Plata, La Plata, Argentina
[b] LIOMM (Laboratorio de Investigaciones en Osteopatías y Metabolismo Mineral), Departamento de Ciencias Biológicas, Facultad de Ciencias Exactas, UNLP, La Plata, Argentina

ARTICLE INFO

Article history:
Received 2 September 2015
Received in revised form 11 November 2015
Accepted 23 November 2015
Available online 23 November 2015

Keywords:
Ultrasound
Polyelectrolyte complex
Scaffolds
Cytotoxicity

ABSTRACT

In recent years, there has been an increasing interest in the design of biomaterials for cartilage tissue engineering. This type of materials must meet several requirements. In this study, we apply ultrasound to prepare a compatibilized blend of polyelectrolyte complexes (PEC) based on carboxymethyl cellulose (CMC) and chitosan (CHI), in order to improve stability and mechanical properties through the inter-polymer macroradicals coupling produced by sonochemical reaction. We study the kinetic of the sonochemical degradation of each component in order to optimize the experimental conditions for PEC compatibilization. Scaffolds obtained applying this methodology and scaffolds without ultrasound processing were prepared and their morphology (by scanning electron microscopy), polyelectrolyte interactions (by FTIR), stability and mechanical properties were analyzed. The swelling kinetics was studied and interpreted based on the structural differences between the two kinds of scaffolds. In addition we evaluate the possible in vitro cytotoxicity of the scaffolds using macrophage cells in culture. Our results demonstrate that the ultrasound is a very efficient methodology to compatibilize PEC, exhibiting improved properties compared with the simple mixture of the two polysaccharides. The test with murine macrophage RAW 264.7 cells showed no evince of cytotoxicity, suggesting that PEC biomaterials obtained under ultrasound conditions could be useful in the cartilage tissue engineering field.

1. Introduction

Biomaterials designed for biomedical applications must meet more stringent requirements than those used for other applications, due to the demands of non-toxicity, degradability and biocompatibility. Based on this premise, in recent years new polysaccharide-based biomaterials with the above mentioned features have been developed [1,2]. Among them, polyelectrolyte complexes (PEC) formed by mixing two oppositely charged polysaccharides in solution without any chemical covalent cross-linker stand out. The main interactions between PEC include strong but reversible electrostatic and dipole–dipole association, as well as hydrogen and hydrophobic bonds [3]. Recently, numerous PEC have found application as carriers for drug delivery, enzyme immobilization, DNA binding, tissue engineering, biosensors, etc [4–8]. In all these cases it is important to notice that the stability of PEC could be affected by many factors including density of charges, degree of ionization, pH of reaction medium, concentration of polyelectrolytes, distribution of ionic groups, molecular weight, mixing ratio, order of reacting polyelectrolytes, and drying process [9].

In order to improve the stability of complexes, different compatibilization strategies of the polyelectrolyte blend could be used as previously reported for other polymer systems [10]. One of these methodologies is based on the use of ultrasound. It is known that low frequency ultrasound operating at high power influences the chemical reactions, not by direct interaction between wave and matter, but due to the cavitation phenomena. Ultrasound also induces structural and chemical changes in the polymer systems as a result of cavitational process [11]. In particular, a remarkable effect of ultrasound on polymers degradation reactions was observed in solution and melt conditions [12–15]. The breakage of molecular chains under ultrasound occurs near the center of the chain and results in formation of macroradicals, as previously demonstrated by Tabata et al. [16]. These macroradicals can further react by transfer processes or by combination, modifying the initial molecular weight distribution. Thus, based on the reactivity of these macroradicals, the ultrasound was employed as a new methodology to improve the compatibility of two incompatible polymer blends. Due to chain scission with macroradicals formation, sonochemically induced reactions can lead to inter-polymer radical coupling and measurable block copolymers which are useful for reactive compatibilization [17–20].

* Corresponding author.

http://dx.doi.org/10.1016/j.ultsonch.2015.11.022
1350-4177/

We have previously prepared a poly(diisopropyl fumarate)/poly (ε-caprolactone) blend obtained by ultrasonic compatibilization through the block copolymer created during sonication [20]. This blend exhibited better surface characteristics than the physical mixtures and its biocompatibility properties were analyzed in view to future applications for bone regeneration. In the present study we used ultrasound methodology in order to improve the compatibility, stability and biological properties of polyelectrolyte complexes based on chitosan (CHI) and carboxymethyl cellulose (CMC), used as scaffolds with potential application in cartilage tissue engineering. For comparison purposes, a blend which had not been submitted to ultrasound was prepared and the morphology, structural stability, swelling behavior, and mechanical properties were analyzed in both kinds of scaffolds. We have also evaluated the possible in vitro cytotoxicity of the scaffolds using macrophage cells in culture.

2. Materials and methods

2.1. Materials

Chitosan (CHI, high molecular weight) and carboxymethyl cellulose (CMC) were purchased from Sigma–Aldrich Argentina. The degree of acetylation (DA) of chitosan, 24%, was assessed by FTIR based on the absorbance ratio at 1320 cm^{-1} and 1456 cm^{-1}, corresponding to amide III and CH_2 bands, respectively, as suggested by Brugnerotto [21].

$$DA(\%) = 31.92(A_{1320}/A_{1456}) - 12.20 \quad (1)$$

The viscosity average molecular weight (M_η) of both polysaccharides was evaluated by capillary viscometry using acetic acid 0.3 M/sodium acetate 0.2 M buffer or sodium chloride 0.2 N as solvent for CHI or CMC, respectively. The measurement temperature was kept at 25.00 ± 0.02 °C. The M_η was evaluated following Eq. (2):

$$[\eta](ml/g) = KM_\eta^a \quad (2)$$

where $[\eta]$ is the intrinsic viscosity and K and a are characteristic parameters for each polymer–solvent system. K and a parameters take values of 0.082 ml/g and 0.76, respectively, for CHI; while 0.043 ml/g and 0.74 were used in the case of CMC [22,23]. Thus, CHI exhibited M_η of 511 kDa, while the corresponding value for CMC was 865 kDa.

2.2. Ultrasonic processing

The ultrasound-delivering equipment was a Bandelin Sonopuls HD 60 apparatus with Titanium flat tip TT 12 accessories and a frequency of 20 kHz. An output power of 37 W was used in all experiments and the temperature of glass vessel with cooling jacket was adjusted at 20.00 ± 0.02 °C using a Lauda Thermostar RCS6. In order to determine the optimal conditions of blend polysaccharides compatibilization, a preliminary assay was carried out using CMC and CHI solution separately. The liquid volume subjected to sonication was 20 ml and the concentration sample was 1.0 wt%. At different times, 1-ml aliquots were removed from the reaction mixture, filtrated through a 0.45-μm Teflon membrane and analyzed by capillary viscometry following the methodology previously described [24].

2.3. Scaffolds preparation

The scaffolds were prepared with a 1.0% w/v CHI solution in 0.25% v/v acetic acid and 1.0% w/v CMC in distilled water. The samples were obtained by dropping the CMC solution into the CHI solution under constant stirring (150 rpm) at 20 °C for 20 min. This time was selected based on the studies of ultrasound degradation of polysaccharides solutions, as previously described in Section 2.2. Under the experimental conditions indicated, pH = 5.0 was attained. One of the samples was compatibilized by applying ultrasound (37 watts) during the dropping (PEC-US) and another one was obtained without ultrasound processing (PEC). Finally, the samples were isolated by discarding the supernatant medium, poured into 24-well plate and freeze-dried until constant weight was achieved.

2.4. Characterization techniques

The surfaces of the matrices were coated with gold and their morphology was examined using scanning electron microscopy (SEM, Philips 505) with an accelerating voltage of 20 kV. In order to evaluate the pore size, the images were analyzed by Soft Imaging System ADDAII, measuring the greatest distance possible between any two points along the boundary of the pore.

Infrared spectroscopy was used to characterize intermolecular interactions between components in the systems. The IR spectra of PEC and PEC-US were recorded with a Nicolet magna ir-560 spectrophotometer by attenuated total reflection (ATR) technique. The spectra were collected over the range of 4000–600 cm^{-1} at a resolution of 4 cm^{-1}.

2.5. Stability and swelling assay

In order to investigate the scaffolds stability with respect to the storage time, samples of PEC and PEC-US were incubated in sterile buffer phosphate (pH = 7.4) at 37 °C for seven days, simulating the physiological conditions,.

The maximum swelling and water absorption capacity of the membranes were determined as previously reported [25]. The water content of the membrane was obtained as the difference between the weight of the water saturated sample (w) and the weight of the initial dried sample (w_0). The percentage of the membrane swelling is defined as:

$$\%S_w = \frac{100(w - w_0)}{w_0} \quad (3)$$

In order to have insights into the water transport process through the membranes, the following equation was used to analyze the swelling process [26]:

$$\frac{W_t}{W_\infty} = kt^n \quad (4)$$

where k is a characteristic constant of the system, which depends on the structural characteristics of the polymer and its interaction with the solvent, n is the swelling exponent, which describes the mechanism of water transport into the membrane, and W_t and W_∞ represent the quantities of absorbed water at time t and at equilibrium time, respectively. The value of n provides information about the water sorption mechanism. If the rate of diffusion of penetrant is the rate limiting, $n = 0.5$ (Fickian kinetics), while a value of n between 0.5 and 1.0 indicates a non-Fickian diffusion process in which the relaxation of polymer chains determines the rate of water sorption. The limit case designed as Case II transport, where $n = 1$ corresponds to a condition in which the rate of water diffusion is higher than the rate of polymer chain relaxation and the rate of mass uptake is directly proportional to time [27]. The value of n and k can be obtained from the slope and intercept of the plot of $\log(W_t/W_\infty)$ versus log t from the experimental data taken up to 60% of the maximum swelling.

2.6. Mechanical testing

The compressive mechanical strength and modulus of elasticity of scaffolds were tested using an universal testing machine (Digimess TC500) with 50 N capacity force load cell under a compression strain rate of 1.3 mm min^{-1}. The measurements were carried out following ASTM D695 norm (room temperature and 50% controlled humidity). The specimens were circular discs of 13 mm diameter and 10 mm thickness. The results presented are the mean values of five independent measurements.

2.7. Cytotoxicity Studies with RAW 264.7 Macrophages

Murine macrophage RAW 264.7 cells were grown in DMEM supplemented with 5% (v/v) FBS and antibiotics (100 U/ml penicillin and 100 g/ml streptomycin) at 37 °C in a 5% CO_2 atmosphere. This cell line has previously been used in our laboratory to assess cytotoxicity since it represents an adequate and sensitive in vitro model for inflammation [28,29]. For the experiments, PEC scaffolds were cut to size, inserted in a 24-well plate, sterilized by immersion in 70% ethanol and irradiated with UV light. The membranes were washed with DMEM, Raw 264.7 macrophages in 10% FBS-DMEM were plated on the scaffolds and incubated for 3 h. After this adhesion incubation period, media was changed to a non serum-containing DMEM without phenol red and incubated for 72 h. In control experiments, macrophages were incubated on standard plastic tissue culture dishes. After the culture period, media were saved for nitric oxide (NO) determination. Cells were washed with PBS, fixed with methanol and stained with Giemsa as we have previously described [29]. The morphology of RAW264.7 cells cultured on both scaffolds was analyzed using a TS100 Eclipse Nikon microscope and photographed with a CCD camera with a 0.7× DXM Nykon lens.

Nitric oxide production was assessed by Griess' reaction [30,31] (using sulfanilic acid as the diazotizing agent and N-1-napthylethylene diamine as the coupling agent). The stable end-product of NO and nitrite released into the culture medium by RAW 264.7 cells was evaluated. Briefly, 400 µl samples of conditioned media or nitrite standards 0–100 nM were mixed with 400 µl of Griess' reagent (1% sulfanilamide and 0.1% naphthylethylene-diamine in 5% phosphoric acid) and absorbance was measured at 530 nm against a blank prepared with non-conditioned medium.

2.8. Statistical analysis

Student's t-test was used for comparisons between the control and experimental groups. All results are expressed as mean ± S.E.M. and represent at least three different experiments performed in triplicate.

3. Results and discussion

3.1. Effect of ultrasound on the polymer solutions

We have previously demonstrated that sonochemical degradation of polymers is an efficient methodology to compatibilize polymer blends, through *in situ* obtention of block copolymer originated by interpolymeric reaction of macroradicals formed by homolytic cleavage of polymer chains [18,20]. In order to determine the optimum compatibilization time for the polysaccharides blend, independent polymer solutions were prepared and submitted to ultrasound degradation as a function of sonication time. Fig. 1 shows the relative change of intrinsic viscosity $[\eta]_t/[\eta]_0$, as a function of the sonication time for CMC and CHI. It can be seen that for both samples a decrease in the degradation rate was observed after 15 min, reaching a $[\eta]_t/[\eta]_0$ value below which no further degradation takes place. This result is in agreement with other sonication studies made using different samples [14,20,32].

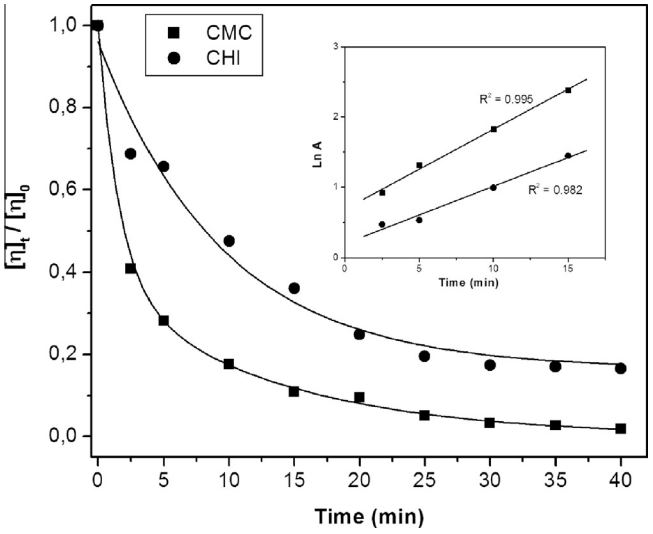

Fig. 1. Evolution of relative changes in intrinsic viscosity of CMC and CHI samples studied as a function of sonication time. The inset presents the degradation kinetic analysis: $lnA = ln([\eta]_0 - [\eta]_\infty)/([\eta]_t - [\eta]_\infty)$ vs time plot and the correlation coefficients (R^2). See Eq. (5).

The kinetic of polysaccharides degradation process was analyzed following the procedure of Li et al. [32]. According to the authors, the kinetics of ultrasonic degradation can be expressed as:

$$[\eta]_t = [\eta]_\infty + ([\eta]_0 - [\eta]_\infty)e^{-kt} \quad (5)$$

where $[\eta]_0$, $[\eta]_t$ and $[\eta]_\infty$ are the intrinsic viscosity at sonication time 0, t and limit intrinsic viscosity, respectively; k is the rate constant of degradation reaction. According to Eq. (5), the magnitude of the rate constant can be evaluated knowing the initial and limit intrinsic viscosity of the polymer solution by plotting a graph of ln(A) against time where $A = ([\eta]_0 - [\eta]_\infty)/([\eta]_t - [\eta]_\infty)$. To estimate the degradation constant rate, only the data before 15 min were used. Inset of Fig. 1 shows this graph for degradation kinetic of CMC and CHI solutions. The kinetic rate constants were 0.114 min^{-1} and 0.082 min^{-1} for CMC and CHI, respectively. Some researchers have explained differences between k values based on the flexibility and/or dissolved stated of polymer chain in aqueous solutions [33]. The two parameters that allows characterizing the conformation and solution behavior of polymers are the persistence length *Lp* and the exponent *a* of Mark-Houwink-Sakurda equation, Eq. (2). *Lp* reflects the linear flexibility of polymer chains in solution and large *Lp* is obtained for the rod-like rigid polymer. *Lp* for CMC and CHI are 11 nm and 15–17 nm, respectively [34,35], which are similar values and characteristic of semiflexible polymer. On the other hand, *a* parameter is a function of the shape of the polymer coil in a solution and is in fact a measure of the interaction of the polymer and solvent. In our systems, the value of *a* is 0.74 and 0.76 for CMC and CHI, respectively, indicating that both polysaccharides exhibited similar solution behavior, as a coil expands in good solvent. Thus, the differences observed for the degradation rate cannot be attributed to the conformational solution behavior. Taking into account that both polysaccharides presented similar structures composed of derived glucose units bound by β-1,4 link (carboxymethyl groups on same glucopyranose or D-glucosamine/N-acetyl-D-glucosamine in CMC or CHI, respectively), we consider that the main difference is the average molecular weight. The CMC which has higher M_η than CHI, exhibited highest rate constant

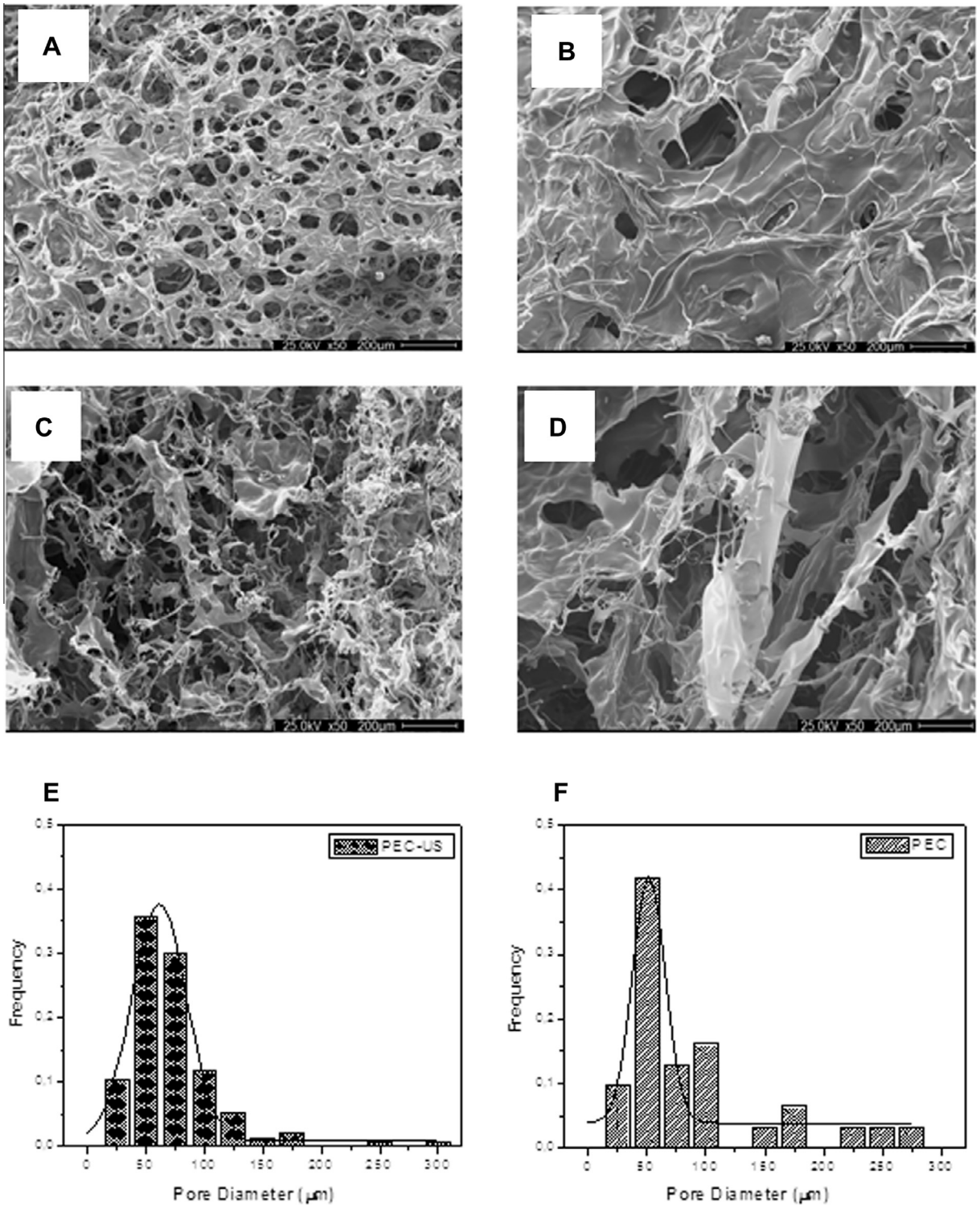

Fig. 2. SEM micrographs of the surface and cross-sectional of PEC-US (A and C) and PEC (B and D), respectively. Pore size distribution of PEC-US (E) and PEC (F) scaffolds.

of degradation. This result is in agreement with those of other previous publications, which demonstrated that the degradation rate decreases with decreasing initial degree of polymerization [14,32].

In a previous study we have shown that a polymer blend under the action of ultrasound degrades at a similar rate at which each of the components is degraded [20]. Based on this fact, we select 20 min as the optimal time for the compatibilization between CMC and CHI.

3.2. Scaffolds characterization

As shown in Section 3.1, we select 20 min as optimum time for ultrasonic compatibilization of the polysaccharide blend. For comparison purposes, a blend of CMC and CHI was prepared without an ultrasound methodology. Both kind of blends were used to obtain the scaffolds and then examined their properties.

The morphology of the PEC-US and PEC scaffolds were analyzed by SEM, as shown in Fig. 2. In both cases, a three-dimensional

highly porous structure with good interconnection between pores and porosities over 70% was observed. Some differences between the surface (Fig. 2A and B, for PEC-US and PEC, respectively) and the inner-structure (Fig. 2C and D for PEC-US and PEC, respectively) of scaffolds were observed, being the more homogenous and less open in the case of PEC-US than PEC scaffolds. For tissue engineering applications, the existence of pores in the polymeric structure is crucial for cell proliferation since they provide adequate conditions for cell migration as well as efficient transport of nutrients and metabolic wastes [36,37]. The quantitative determination of the pore size showed that the mean pore diameter of the scaffolds was 82 ± 7 μm and 115 ± 9 μm for PEC-US and PEC, respectively. These values are in the range of 50 to 300 μm as reported in the literature for other freeze-dried matrices [37,38]. On the other hand, the pore size distribution (Fig. 2E and F for PEC-US and PEC, respectively) shows that in the scaffold treated with ultrasound the pore distribution is more uniform and the pores are well distributed between the surface and the inner-structure. This fact can be due to the better interaction between CMC and CHI in the PEC-US scaffold, favored by the process that takes place during the ultrasound application. More evidence of this effect was obtained by FTIR analysis.

FTIR spectra of CHI, CMC and PEC obtained by ultrasound process and without ultrasound are shown in Fig. 3 (wavelength 1800–700 cm^{-1}). Chitosan spectrum shows two typical bands at 1640 and 1556 cm^{-1} attributed to amide I and amide II, respectively [39]. In addition, the bands at 1152 cm^{-1} and 1377 cm^{-1} are assigned to stretching vibration of C—N and bending vibration of O—H, respectively. In the spectrum of CMC, two strong peaks at 1590 and 1420 cm^{-1} were observed due to the asymmetrical and symmetrical stretching of —COO^- groups. The FTIR spectra of PEC obtained only by mixture of CHI and CMC exhibited a decrease in the intensity of the amide I (1640 cm^{-1}) in relation to amide II absorption band (1556 cm^{-1}), together with a displacement of the —COO^- group absorption band at 1410 cm^{-1}, suggesting ionic interaction between the two polysaccharides, as reported by others researches [40,41]. On the other hand, when the PEC was obtained under ultrasound conditions the FTIR spectrum presented some differences: the amide I absorption band at 1640 cm^{-1} can be seen as a shoulder and a strong band at 1593 cm^{-1} appeared, which is assigned to asymmetric flexion of —NH_3^+ and carboxylate groups, while the symmetrical stretching of —COO^- groups shift to 1416 cm^{-1}. Besides, a new weak but visible band appears at 1727 cm^{-1}, assignable to stretching vibration of >C=O ester group which could be formed by sonochemistry reaction, as previously demonstrated for another system [42]. Fig. 4 shows this band is absent in the spectrum of PEC obtained without ultrasound, suggesting that new covalent bonds, which improve the polysaccharide compatibility exist between CHI and CMC.

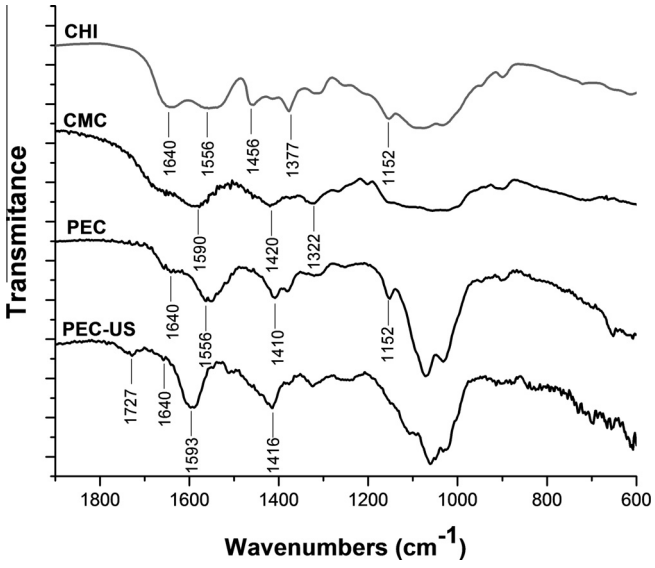

Fig. 3. FTIR spectra (from 1800 to 600 cm^{-1}) of chitosan (CHI), carboxymethyl cellulose (CMC), polyelectrolyte complex of CHI and CMC without ultrasound (PEC) and with ultrasound methodology (PEC-US).

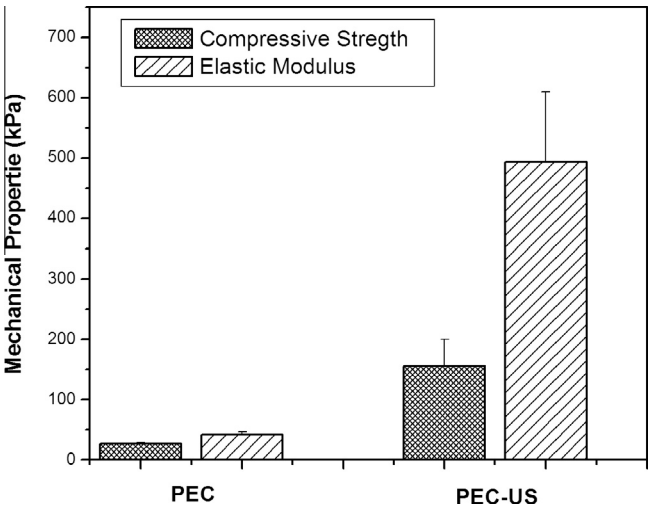

Fig. 4. Compressive strength and elastic modulus of PEC and PEC-US scaffolds. The results presented are the mean values of five independent measurements.

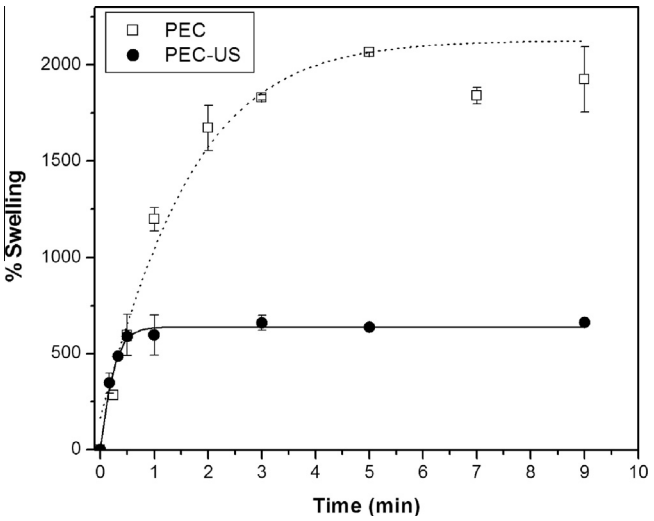

Fig. 5. Percentage of swelling of PEC and PEC-US scaffolds as a function of time at 37 °C in buffer phosphate pH = 7.4.

3.3. Mechanical properties

With the purpose of evaluating the mechanical properties of scaffolds, which are relevant to *in vivo* interaction, in view of their future biomedical applications, the mechanical behavior of PEC scaffolds was evaluated by compressive tests. Compressive strength (CS) and elastic modulus (EM) were measured for PEC and PEC-US. Fig. 4 shows that the PEC-US exhibited higher compressive strength and elastic moduli which are one order of magnitude greater than those for PEC (155.7 ± 44.1 kPa vs 27.5 ± 1.7 kPa and 493 ± 117 kPa vs 42 ± 5 kPa for CS and EM, respectively). These

results are consistent with the morphology of the scaffolds observed by SEM. The resistance of the scaffolds increases when the pore diameter decreases and the pore distribution is more homogeneous, as obtained for PEC-US scaffold. Similar compressive strength value for other PEC based on chitosan/gelatin or chitosan/alginate was previously reported [43,44]. The scaffold must provide to cells a 3D structure and mechanical support for their attachment and proliferation, allowing them to grow into a functional tissue-engineered construct [45]. In particular, biomaterials applied to the repair of damaged cartilage must have similar mechanical properties to this kind of tissue. According to previous studies Young's modulus of cartilage ranged from 450 to 800 kPa [45,46]. Thus, our results demonstrate that PEC-US scaffold exhibited elastic modulus which is appropriate for cartilage tissue engineering.

3.4. Scaffold stability and swelling behavior

In order to evaluate the structural integrity of the PEC and PEC-US scaffolds, samples of both types of scaffolds were immersed in PBS during seven days. The PBS was then extracted and the samples were dried and weighted. The percent of weight loss was 52.8 ± 4.3% and 24.6 ± 3.9% for PEC and PEC-US, respectively. This result shows that PEC-US scaffold has a stronger structural stability than that of PEC scaffold, due to the better compatibility between the two polyelectrolyte submitted to ultrasound process.

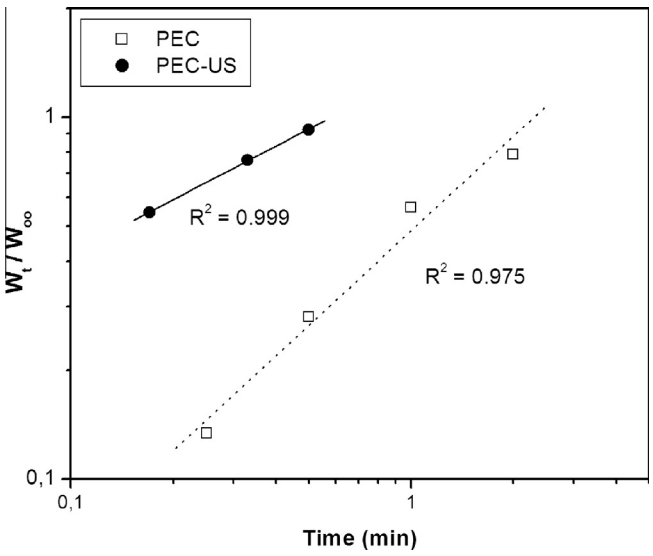

Fig. 6. Double logarithmic plot between W_t/W_∞ and time at initial stage, derived of Fig. 5, for PEC and PEC-US scaffolds.

Fig. 5 presents the swelling kinetics of the PEC scaffolds in buffered aqueous solutions of pH 7.4 at 37 °C. It can be observed that the swelling behavior of both samples is similar: the degree of swelling increases overtime until a certain point when it becomes constant, reaching equilibrium within 3 or 1 min for PEC and PEC-US, respectively. However, the maximum swelling attained was highly different for the two scaffolds analyzed; 2066% and 638%, for PEC and PEC-US, respectively. This result demonstrates that the scaffold swelling ability is strongly affected by ionic crosslinking and the covalent interaction originated during the ultrasound compatibilization of PEC-US.

The hydrogel swelling mechanism can be interpreted through the two processes, concentration gradient-controlled diffusion and relaxation-controlled swelling; both of them contribute to the rate and extent of penetrant sorption into the polymer [47]. As previously mentioned, to determine the *n* exponent the kinetics of such process could be analyzed through the Fick model (Eq. (4)). Thus, a plot of $\log(W_t/W_\infty)$ versus log t (Fig. 6) allowed us to estimate the *n* values for PEC-US and PEC as 0.49 and 0.87, respectively. These results suggest that in the first scaffold the mechanism of water transport is controlled by a Fickian diffusion process, while in the PEC scaffold the rate of water transport responds to a non-Fickian diffusion process, which depends of diffusion and of the macromolecular chain relaxation. Our results are in good agreement with those presented by Kim et al. [47] for chitosan-hyaluronic acid polyelectrolyte complexes and by Giers zewska-Drużyńska et al. [48] for chitosan-alginate membranes.

3.5. Cytotoxicity evaluation

We investigate if our scaffolds might generate any cytotoxic effect on cultures of Raw 264.7 macrophages. Macrophages act during inflammation of wound healing and against bacterial infections, and thus represent a good model to investigate cytotoxicity. Fig. 7 shows the presence of macrophages at different levels of the PEC-US and PEC matrixes (Fig. 7A and B) regardless the

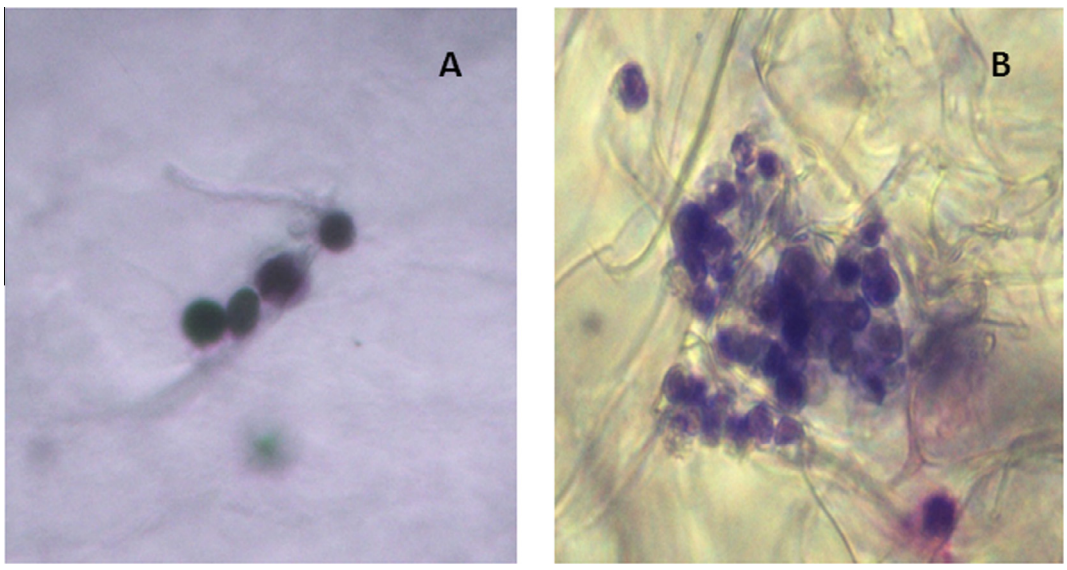

Fig. 7. Morphology of RAW 264.7 macrophages. Cells stained with Giemsa after 72 h of culture on PEC-US (A) and PEC (B). Magnification ×100.

Table 1
Nitric oxide (NO) produced by RAW 264.7 macrophages cultured on standard plastic tissue culture dishes (control), PEC-US and PEC scaffolds.

Sample	NO [nmol/mL]
Plastic control	3.83 ± 0.41
PEC-US	4.24 ± 0.53
PEC	3.36 ± 0.51

Results are expressed as X ± SEM.

compatibilization procedure. Cells seem to maintain their round morphology without cytoplasmic extensions, 72 h after culture. As we have previously reported, when these cells are exposed to lipopolysaccharide (LPS) as a positive control of cytotoxicity, they show an expanded and vacuolated cytoplasm with several extensions, suggesting activation of the macrophages [28]. In addition, we have evaluated the potential cytotoxicity by the release of NO to the culture media. Table 1 shows that the NO production was similar when cells had been grown on control tissue culture plastic or into either PEC-US or PEC scaffolds.

Recent studies have suggested that chitosan could develop toxic effects. For instance, cytotoxicity was found to be induced by chitosan on macrophage when used as poly(lactide-co-glycolic) (PLGA) nanoparticle stabilizer [49] or in hybrid hydrogels, where it induces TNF-α and NO production by RAW 264.7 macrophages [50]. In our previous report, in chitosan-based matrix did not show any sign of toxicity on osteoblastic lines [39]. On the other hand, no cytotoxic effect has been reported for carboxymethyl cellulose [51]. Thus, our present results demonstrate that both PEC-US and PEC exerted no in vitro cytotoxicity on Raw 264.7 macrophages.

4. Conclusions

In the present work the ultrasonic degradation of chitosan and carboxymethyl cellulose was analyzed in order to find the optimal conditions for compatibilizing a blend of both polysaccharides. The kinetic of the process show that CMC solution exhibited higher rate constant of degradation than CHI solution, which was attributed to the highest viscosity average molecular weight of CMC. SEM and FTIR analysis demonstrated that the scaffold obtained applying ultrasound during their preparation presented a more homogenous surface and pore size distribution, in comparison to those obtained without ultrasound. This result indicated that covalent link between the two polysaccharides were achieved due to macroradical sonochemical reactions. The structural differences between PEC-US and PEC scaffolds allow us to explain highest elastic moduli (close to cartilage) and strongest stability at pH = 7.4 of PEC-US. Also, the swelling mechanism was different for the two scaffolds, as a result of the structural differences. PEC-US exhibited a diffusive water transport mechanism, while PEC swelling behavior is a non-Fickian diffusion process controlled by diffusion and relaxation of polymer chains. Both PEC-US and PEC evidence no cytotoxicity as proved by macrophage cells, indicating that these materials could be useful in cartilage tissue regeneration.

Acknowledgements

This work was partially supported by grants from Facultad de Ciencias Exactas, Universidad Nacional de La Plata (UNLP, 11/X644; 11/X643) and Comisión de Investigaciones Científicas de la Provincia de Buenos Aires (CICPBA). We thank Ms. María Cecilia Moreno for the revision and improvement of the language of this paper. MSB is Investigador Asistente of CONICET, LFM is Doctoral Fellow of CONICET, AMC is a member of the Carrera del Investigador Científico de la CICPBA, MSC a fulltime Researcher and Professor of UNLP.

References

[1] N.B. Shelke, R. James, C.T. Laurencin, S.G. Kumbar, Polysaccharide biomaterials for drug delivery and regenerative engineering, Polym. Adv. Tech. 25 (2014) 448–460.
[2] P. Laurienzo, J.C. Fernandes, S. Colliec-Jouault, J.H. Fitton, The use of natural polysaccharides as biomaterials, Biomed. Res. Int. 2015 (2015) 242378–242379.
[3] A.V. Il'ina, V.P. Varlamov, Chitosan-based polyelectrolyte complexes: a review, Appl. Biochem. Microbiol. 41 (2005) 5–11.
[4] J.H. Hamman, Chitosan based polyelectrolyte complexes as potential carrier materials in drug delivery systems, Mar. Drugs 8 (2010) 1305–1322.
[5] F. Kara, G. Demirel, H. Tümtürk, Immobilization of urease by using chitosan-alginate and poly(acrylamide-co-acrylic acid)/kappa-carrageenan supports, Bioprocess Biosyst. Eng. 29 (2006) 207–211.
[6] Y. Wen, L. Grøndahl, M.R. Gallego, L. Jorgensen, E.H. Møller, H.M. Nielsen, Delivery of Dermatan sulfate from polyelectrolyte complex-containing alginate composite microspheres for tissue regeneration, Biomacromolecules 13 (2012) 905–917.
[7] N. Cifani, L. Chronopoulou, B. Pompili, A. Di Martino, F. Bordi, S. Sennato, E.G. Di Domenico, C. Palocci, F. Ascenzioni, Improved stability and efficacy of chitosan/pDNA complexes for gene delivery, Biotechnol. Lett. 37 (2015) 557–565.
[8] M. Yang, Y. Yang, B. Liu, G. Shen, R. Yu, Amperometric glucose biosensor based on chitosan with improved selectivity and stability, Sens. Actuators B 101 (2004) 269–276.
[9] Y. Luo, Q. Wang, Recent development of chitosan-based polyelectrolyte complexes with natural polysaccharides for drug delivery, Int. J. Biol. Macromol. 64 (2014) 353–367.
[10] B. Imre, B. Pukánszky, Compatibilization in bio-based and biodegradable polymer blends, Eur. Polym. J. 49 (2013) 1215–1233.
[11] K.S. Suslick, G.J. Price, Application of ultrasound to material chemistry, Annu. Rev. Mater. Sci. 29 (1999) 295–326.
[12] J.R. Thomas, Sonic degradation of high polymers in solution, J. Phy. Chem. 63 (1959) 1725–1729.
[13] G.J. Price, P.F. Smith, Ultrasonic degradation of polymer solutions-III. the effect of changing solvent and solution concentration, Eur. Polym. J. 29 (1993) 419–424.
[14] M. Marx-Figini, Studies on the ultrasonic degradation of cellulose. Macromolecular properties, Die Ang. Makromol. Chem. 250 (1997) 85–92.
[15] C. Ávila-Orta, C. Espinoza-González, G. Martínez-Colunga, D. Bueno-Baqués, A. Maffezzoli, F. Lionetto, An overview of progress and current challenges in ultrasonic treatment of polymer melts. An overview of progress and current challenges in ultrasonic treatment of polymer melts, Adv. Polym. Tech. 32 (S1) (2012) E582–E602.
[16] M. Tabata, T. Miyazawa, O. Kobayashi, J. Sohma, Direct evidence of main-chain scissions induced by ultrasonic irradiation of benzene solutions of polymers, Chem. Phys. Lett. 73 (1980) 178–180.
[17] W. Feng, A.I. Isayev, In-situ compatibilization of PP/EPDM blends during ultrasound aided extrusion, Polymer 45 (2004) 1207–1216.
[18] A.H. Lebovitz, M.K. Gray, A.C. Chen, J.M. Torkelson, Interpolymer radical coupling reactions during sonication of polymer solutions, Polymer 44 (2003) 2823–2828.
[19] J.S. Oh, A.I. Isayev, M.A. Rogunova, Continuous ultrasonic process for in situ compatibilization of polypropylene/natural rubber blends, Polymer 44 (2003) 2337–2349.
[20] J.M. Fernández, M.S. Molinuevo, A.M. Cortizo, A.D. McCarthy, M.S. Cortizo, Characterization of poly(ε-caprolactone)/polyfumarate blends as scaffolds for bone tissue engineering, J. Biomat. Sci. 21 (2010) 1297–1312.
[21] J. Brugnerotto, J. Lizardi, F.M. Goycoolea, W. Argüelles Monal, J. Desbriéres, M. Rinaudo, An infrared investigation in relation with chitin and chitosan characterization, Polymer 42 (2001) 3569–3580.
[22] M. Rinaudo, M. Milas, P. Le Dung, Characterization of chitosan. Influence of ionic strength and degree of acetylation on chain expansion, Int. J. Biol. Macromol. 15 (1993) 281–285.
[23] W. Brown, D. Henley, Studies on cellulose derivatives. Part IV. The configuration of the polyelectrolyte sodium carboxymethyl cellulose in aqueous sodium chloride solutions, Die Makromol. Chem. 79 (1964) 68–88.
[24] J.M. Giussi, P.E. Allegretti, M.S. Cortizo, New Copolymers of a Tautomerizable β-Ketonitrile Monomer: Synthesis, Characterization and Solution Tautomerism, J. Polym. Sci. Part A: Polym. Chem. 50 (2012) 4161–4169.
[25] M. Pasqualone, T.G. Oberti, H.A. Andreetta, M.S. Cortizo, Fumarate copolymers-based membranes overlooking future transdermal delivery devices: synthesis and properties, J. Mater. Sci. Mater. Med. 24 (2013) 1683–1692.
[26] L. Ritger, N.A. Peppas, A simple equation for description of solute release. I. Fickian and non-Fickian release from non-swellable devices in the form of slabs, spheres, cylinders or discs, J. Control. Release 5 (1987) 23–26.
[27] F. Ganji, S. Vasheghani-Farahani, E. Vasheghani-Farahani, Theoretical description of hydrogel swelling: a review, Iranian Polym. J. 19 (2010) 375–398.
[28] J.M. Fernandez, M.S. Cortizo, A.M. Cortizo, Fumarate/Ceramic composite based scaffolds for tissue engineering: evaluation of hydrophylicity, degradability, toxicity and biocompatibility, J. Biomater. Tissue Eng. 4 (2014) 227–234.
[29] A.M. Cortizo, G. Ruderman, G. Correa, I.G. Mogilner, E.J. Tolosa, Effect of surface topography of collagen scaffolds on cytotoxicity and osteoblast differentiation, J. Biomater. Tissue Eng. 2 (2012) 125–132.

[30] M.S. Molinuevo, S.B. Etcheverry, A.M. Cortizo, Macrophage activation by a vanadyl–aspirin complex is dependent on L-type calcium channel and the generation of nitric oxide, Toxicology 210 (2005) 205–212.
[31] A.M. Cortizo, M. Caporossi, G. Lettieri, S.B. Etcheverry, Vanadate-induced nitric oxide production: role in osteoblast growth and differentiation, Eur. J. Pharmacol. 400 (2000) 279–285.
[32] Y. Li, J. Li, S. Guo, H. Li, Mechanochemical degradation kinetics of high-density polyethylene melt and its mechanism in the presence of ultrasonic irradiation, Ultrason. Sonochem. 12 (2005) 183–189.
[33] S. Koda, K. Taguchi, K. Futamura, Effects of frequency and a radical scavenger on ultrasonic degradation of water-soluble polymers, Ultrason. Sonochem. 18 (2011) 276–281.
[34] C.W. Hoogendam, A. de Keizer, M.A. Cohen Stuart, B.H. Bijsterbosch, J.A.M. Smit, J.A.P.P. van Dijk, P.M. van der Horst, J.G. Batelaan, Macromolecules 31 (1998) 6297–6309.
[35] M. Rinaudo, Chitin and chitosan: properties and applications, Prog. Polym. Sci. 31 (2006) 603–632.
[36] P. Coimbra, P. Alves, T.A.M. Valente, R. Santos, I.J. Correia, P. Ferreira, Sodium hyaluronate/chitosan polyelectrolyte complex scaffolds for dental pulp regeneration: synthesis and characterization, Int. J. Biol. Macromol. 49 (2011) 573–579.
[37] J.V. Araujo, N. Davidenko, M. Danner, R.E. Cameron, S.M. Best, Novel porous scaffolds of pH responsive chitosan/carrageenan-based polyelectrolyte complexes for tissue engineering, J. Biomed. Mater. Res. Part A 102 (2014) 4415–4426.
[38] N. Annabi, J.W. Nichol, X. Zhong, C. Ji, S. Koshy, A. Khademhosseini, F. Dehghani, Controlling the porosity and microarchitecture of hydrogels for tissue engineering, Tissue Eng. Part B 16 (2010) 371–383.
[39] M.S. Berghoff, A.M. Cortizo, Cortizo, Interaction studies of mixed matrices of chitosan-poly-ε-caprolactone and alendronate for bone tissue engineering, Adv. Chitin Sci. 11 (2009) 88–92.
[40] C. Tapia, Z. Escobar, E. Costa, J. Sapag-Hagar, F. Valenzuela, C. Basualto, M.N. Gai, M. Yazdani-Pedram, Comparative studies on polyelectrolyte complexes and mixtures of chitosan-alginate and chitosan-carrageenan as prolonged diltiazem clorhydrate release systems, Eur. J. Pharm. Biopharm. 57 (2004) 65–75.
[41] Q. Zhao, J. Qian, Q. An, C. Gao, Z. Gui, H. Jin, Synthesis and characterization of soluble chitosan/sodium carboxymethyl cellulose polyelectrolyte complexes and the pervaporation dehydration of their homogeneous membranes, J. Membr. Sci. 333 (2009) 68–78.
[42] C.B. Hobuss, D. Venzke, B.S. Pacheco, A.O. Souza, M.A.Z. Santos, S. Moura, F.H. Quina, K.G. Fiametti, J.V. Oliveira, C.M.P. Pereira, Ultrasound-assisted synthesis of aliphatic acid esters at room temperature, Ultrason. Sonochem. 19 (2012) 387–389.
[43] Y.J. Yin, K.D. Yao, G.X. Cheng, J.B. Ma, Properties of polyelectrolyte complex films of chitosan and gelatin, Polym. Int. 48 (1999) 429–433.
[44] C. Ceccaldi, R. Bushkalova, C. Alfarano, O. Lairez, D. Calise, P. Bourin, C. Frugier, C. Rouzaud-Laborde, D. Cussac, A. Parini, B. Sallerin, S.G. Fullana, Evaluation of polyelectrolyte complex-based scaffolds for mesenchymal stem cell therapy in cardiac ischemia treatment, Acta Biomater. 10 (2014) 901–911.
[45] C.J. Little, N.K. Bawolin, X. Chen, Mechanical properties of natural cartilage and tissue-engineered constructs, Tissue Eng. Part B 17 (2011) 213–227.
[46] J.M. Mansour, Biomechanics of cartilage, in: C. Oatis (Ed.), Kinesiology: The Mechanics and Pathomechanics of Human Movement, Lippincott Williams and Wilkins, Philadelphia, PA, 2003, pp. 66–79.
[47] S.J. Kim, K.J. Lee, S.I. Kim, Swelling behavior of polyelectrolyte complex hydrogels composed of chitosan and hyaluronic acid, J. Appl. Polym. Sci. 93 (2004) 1097–1101.
[48] M. Gierszewska-Drużyńska, J. Ostrowska-Czubenko, Mechanism of water diffusion into noncrosslinked and ionically crosslinked chitosan membranes, Prog. Chem. Appl. Chitin Deriv. XVII (2012) 59–66.
[49] N. Grabowski, H. Hillaireau, J. Vergnaud, N. Tsapis, M. Pallardy, S. Kerdine-Römer, E. Fattal, Surface coating mediates the toxicity of polymeric nanoparticles towards human-like macrophages, Int. J. Pharm. 482 (2015) 75–83.
[50] M. He, A. Potuck, Y. Zhang, C.C. Chu, Arginine-based polyester amide/polysaccharide hydrogels and their biological response, Acta Biomater. 10 (2014) 2482–2494.
[51] P. Kollar, V. Závalová, J. Hošek, P. Havelka, T. Sopuch, M. Karpíšek, D. Třetinová, P. Suchý Jr., Cytotoxicity and effects on inflammatory response of modified types of cellulose in macrophage-like THP-1 cells, Int. Immunopharmacol. 11 (2011) 997–1001.